lene glycol-*bis*(2-aminoethyl)-*N,N,N,N*-tetraacetic acid (EGTA) (Ca^{2+}-free BSS).

Construction of Lentivirus Vectors Expressing Interfering Short Hairpin RNA (shRNAi) and Microglial Transduction

Lentivirus containing shRNAi was prepared by the method previously described (Yogosawa et al., 2005). The self-inactivating (SIN) vector construct pCS-RfA-CG, which contains the EGFP gene under the control of the CMV promoter and sites for site-specific recombination with a Gateway vector (attR1,2), was used for simultaneous expression of EGFP and shRNA. Plasmid containing $P2X_4R$ shRNAi under the control of human U6 promoter was provided by Dr. K. Inoue (Kyushu Univ. Fukuoka, Japan). The gene of the $P2X_4R$ shRNAi-expressing cassette inserted into pENTR™1A was transferred into the pCS-RfA-CG by a recombination reaction using Gateway LR Clonase (Invitrogen). The sequence of shRNA targeted for firefly luciferase was used as a control (Nishitsuji et al., 2004). The sequence was inserted into the piGENE™ hU6 *Bsp*MI vector (iGENE Therapeutics, Tsukuba, Japan), and the gene of the luciferase shRNAi-expressing cassette was ligated into the pCS-RfA-CG. The sequence of $shP2X_4R$ was: 5′-GGG ATA AGA GAT ATA GGT AAC GTG TGC TGT CCG TTA CTT ATA TTT CTT GTC CCT TTT T-3′. We confirmed the specificity of P2×4R shRNAi by a coexpression assay. pCS-shP2×4R-CG was cotransfected into Cos7 cells with P2×4 expression plasmid (provided by Dr. K. Inoue) or HA-tagged P2Y12R plasmid (Supplemental information). pCS-shP2×4R-CG significantly suppressed P2×4R expression but had no effect P2Y12R expression. The recombined plasmid was cotransfected into 293FT cells (Invitrogen) with a packaging plasmid (pCAG-HIVgp) and a plasmid expressing Rev and vesicular stomatitis virus G glycoprotein (pCMV-VSV-G-RSV-Rev), and the supernatant was collected after 48 h and filtered through a 0.45-μm pore filter (Falcon). Viral particles in the supernatant were concentrated by ultracentrifugation for 2 h at 19,400 rpm (SW28 rotor; Beckmann Coulter, CA) and recovered by suspension in Hanks buffered saline (Invitrogen).

The recombinant lentivirus (2×10^5 infectious units) was added to the mixed glial cells that had been cultured for 12 days in a 25-cm^2 flask, and cultured for 6 days in DMEM containing 10% FCS. Floating cells were collected as microglia and allowed to attach to appropriate dishes or glasses. The efficiency of microglia transduction with the $shP2X_4R$ vector was 20–30%, the same as with the shControl vector according to an analysis of the number of microglia expressing EGFP by flow cytometry.

Isolation of EGFP-Positive Microglia

After transduction with the lentivirus vectors, floating cells collected as microglia were resuspended in PBS containing 2% FCS. EGFP-positive and -negative cells were sorted with a FACSVantageSE flow cytometry system (BD Biosciences). Live gating was performed with propidium iodide (Sigma-Aldrich, St. Louis, MO). The purity of the EGFP-positive cells was >99% according to a flow cytometry analysis.

Western Blot Analysis of P2X Receptor Expression

Sorted cells were lysed in SDS sample buffer. $P2X_4R$, $P2X_7R$, EGFP, and actin proteins in the lysate equivalent to 2×10^4 cells were separated by 10% SDS-PAGE and detected by Western blot analysis with 1 μg/mL anti-$P2X_4R$ antibody (Alomone Labs, Jerusalem, Israel), 0.6 μg/mL anti-$P2X_7R$ (Alomone Labs), anti-GFP antibody (diluted 1:1,000, Medical & Biological Laboratories, Nagoya, Japan), and anti-actin antibody (diluted 1:1,000, Sigma), respectively, and visualized with the ECL system.

RT-PCR Analysis for $P2Y_{12}R$ Gene Transcripts

RNA was isolated from the sorted cells with the RNeasy Mini Kit (QIAGEN, Hildem, Germany) containing a DNase treatment, according to the manufacturer's protocols. Reverse transcription of RNA was performed with SuperScript III reverse transcriptase (Invitrogen). The PCR amplification conditions were 30 s at 94°C, 15 s at 60°C, and 30 s at 68°C for 25–35 cycles, except for the initial denaturation step of 2 min at 94°C and the final cycle with an elongation step of 5 min at 68°C. An extra reaction mixture without reverse transcriptase was used as a control for DNA contamination of the RNA sample. The primers used were as follows: rat $P2Y_{12}R$, 5′-AAA CTT CCA GCC CCA GCA ATC T-3′ (forward), 5′-CAA GGC AGG CGT TCA AGG AC-3′ (reverse); rat β-actin, as an internal standard, 5′-TTG TTA CCA ACT GGG ACG ACA TGG-3′ (forward), 5′-GAT CTT GAT CTT CAT GGT GCT AGG-3′ (reverse). PCR products of 447 bp for $P2Y_{12}R$ and 763 bp for β-actin were analyzed on a 1.5% agarose and stained with ethidium bromide. The relative intensity of the bands for $P2Y_{12}R$ was quantified by densitometry with NIH image software and normalized to the β-actin products. The normalized values were used to calculate the ratio of $P2Y_{12}R$ mRNA level in the EGFP-positive cells transduced with the $shP2X_4R$ vector to the level in the EGFP-positive cells transduced with the shControl vector.

Calcium Imaging

The intracellular calcium concentration ($[Ca^{2+}]_i$) was monitored by the fura-2 method described by Inoue et al. (1998), using a highly sensitive intensifier target video camera C2400 and an Argus 50 image processor (Hama-

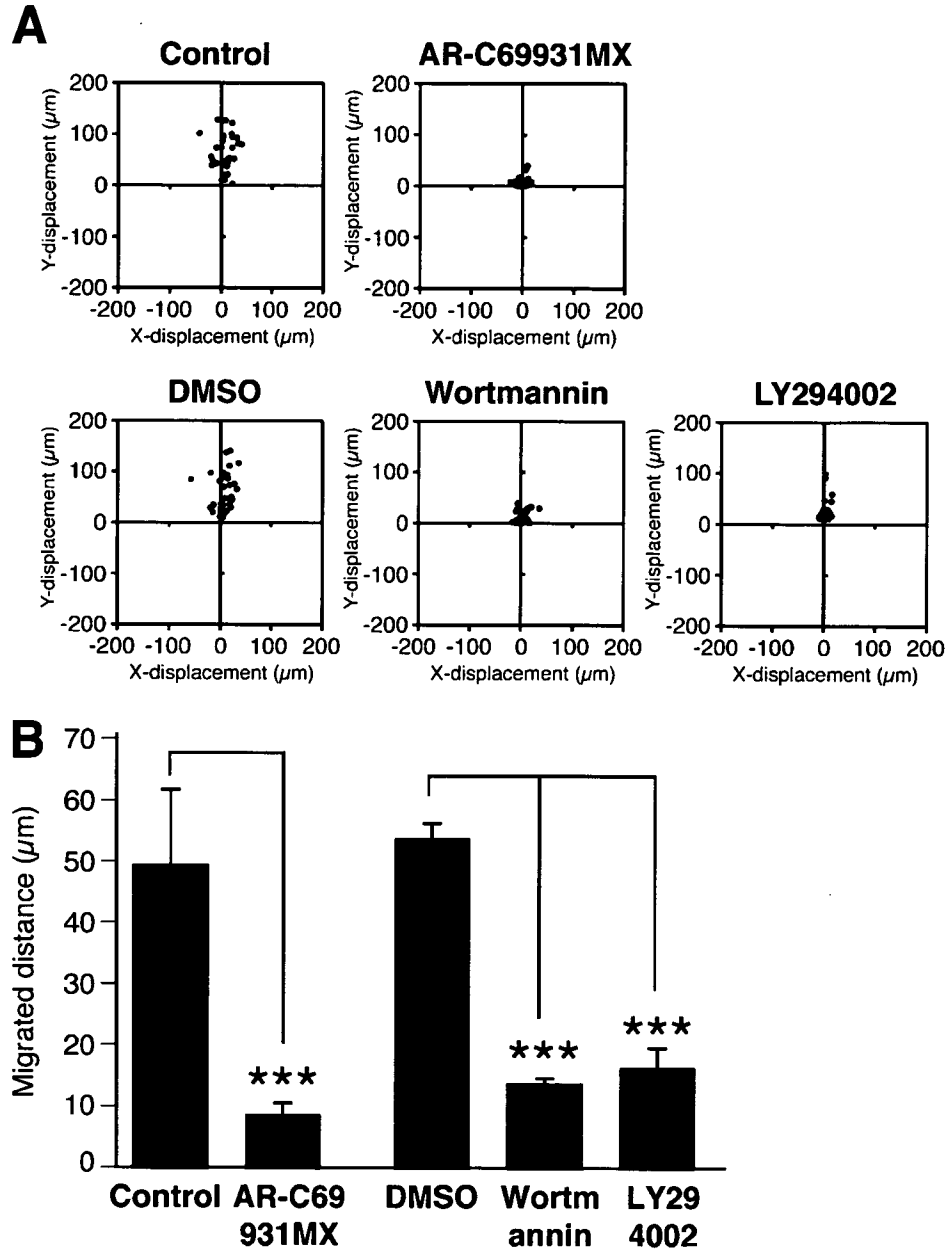

Fig. 1. Effect of PI3K inhibitors on ATP-induced microglial chemotaxis. (**A**) Microglia were pretreated with 1 μM AR-C69931MX for 10 min or with 0.125% DMSO, 100 nM wortmannin, or 50 μM LY294002 for 20 min, and microglial migration towards 50 μM ATP was observed in the Dunn chemotaxis chamber. The distance and direction migrated by individual cells are shown as x and y coordinates on scatter diagrams. The position of the outer well of the chamber is at the top in the vector diagrams of cells. (**B**) Chemotaxis by each cell was quantified by measuring the (x, y) distance migrated from the starting position. Data are means ± SD of three independent experiments. $^{***}P < 0.001$, Student's t-test.

matsu Photonics). Microglia transduced with the lentivirus vectors were plated at 2×10^5 cells/well on poly-L-lysine-coated CELLocate microgrid coverslips (Eppendorf, Hambrug, Germany). After 2 h, the cells were incubated with 10 μM fura-2 acetoxymethylester (fura-2/AM, Dojindo Laboratories, Kumamoto, Japan) at 37°C for 30 min in DMEM containing 25 mM HEPES (DMEM-H, Invitrogen), and the coverslips were mounted on an inverted epifluorescence microscope (TMD-300, Nikon, Tokyo, Japan). The cells were exposed to drugs dissolved in DMEM-H by superfusion. Raw data were recorded as 500-nm emissions of fura-2 excited alternately at 340 and 380 nm, and $[Ca^{2+}]_i$ was expressed as the ratio of the fluorescence intensity at 340 nm to the fluorescence intensity at 380 nm (F340/380).

RESULTS

Involvement of the PI3K Pathway in ATP-Induced Microglial Chemotaxis

We previously reported that ATP-induced microglial membrane ruffling were inhibited by treatment with pertussis toxin and a P2Y$_{12}$R-selective antagonist, AR-C69931MX, suggesting that Gi/o-coupled P2Y$_{12}$R is involved in both the membrane ruffling and the chemotaxis (Honda et al., 2001). Stimulation of P2Y$_{12}$R has been reported to induce PI3K activation (Czajkowski et al., 2004; Soulet et al., 2004; Van Kolen and Slegers, 2004). To determine whether PI3K activation is required for chemotaxis by ATP-stimulated microglia, we investigated the effects of the PI3K inhibitors wortmannin and

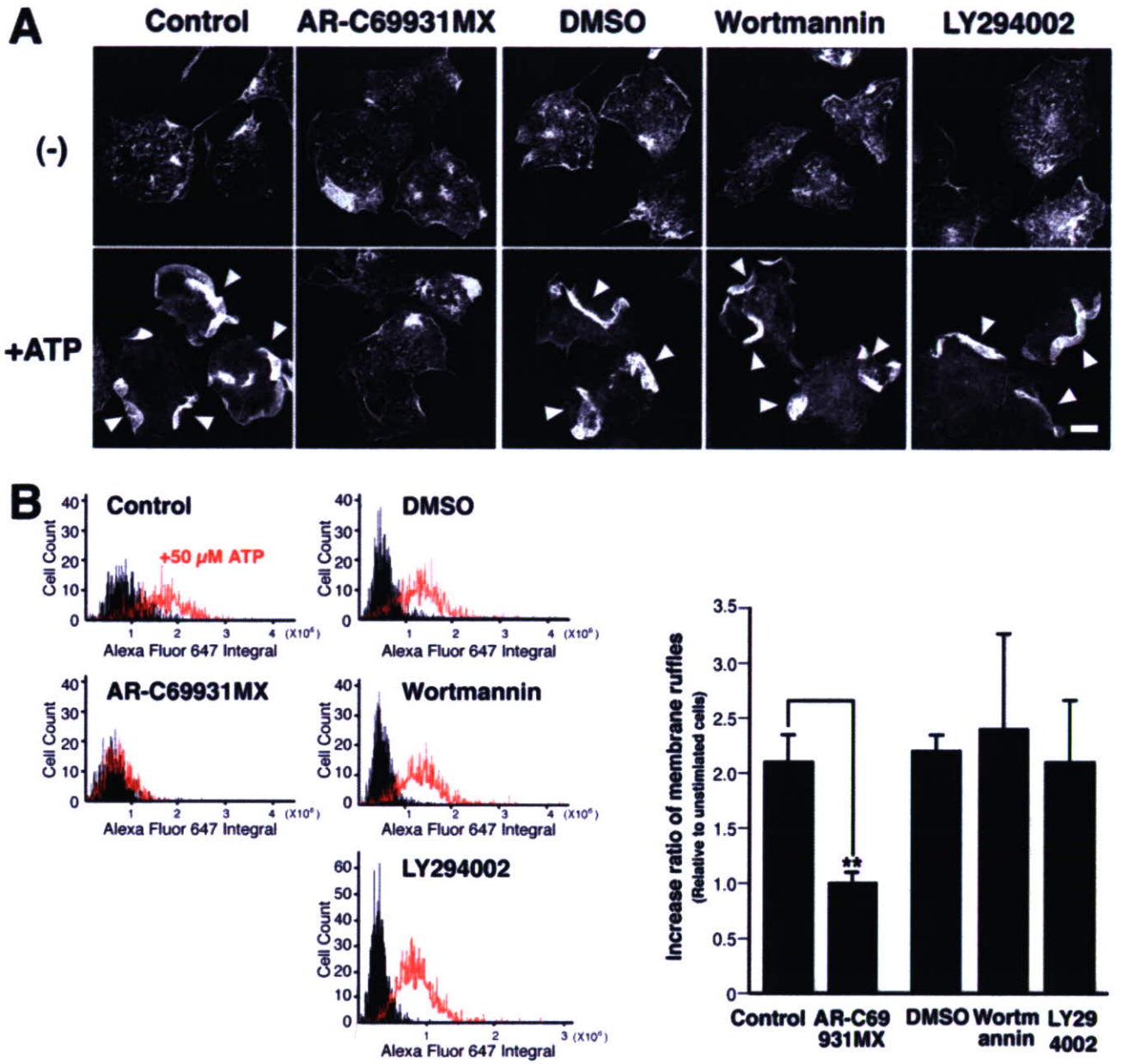

Fig. 2. Effect of PI3K inhibitors on ATP-induced microglial membrane ruffling. (**A**) Microglia were pretreated with 1 μM AR-C69931MX, 0.125% DMSO, 100 nM wortmannin, or 50 μM LY294002 as described in Fig. 1A, and then stimulated with 50 μM ATP for 5 min. After fixation, the cells were stained with Texas Red-conjugated phalloidin to visualize membrane ruffles. Arrowheads indicate membrane ruffles. Scale bar, 10 μm. (**B**) Quantification of membrane ruffles. Microglia were stimulated as in A for 5 min, fixed, and stained with an anti-Iba1 antibody and Alexa Fluor 647-conjugated phalloidin to recognize individual microglial cells and membrane ruffles, respectively. The F-actin content of microglial cells was quantified as integral intensity of Alexa Fluor 647 fluorescence by using LSC. The five panels on the left side are histograms representing the total F-actin in each cell (*x*-axis, Alexa fluor 647 integral) and the number of scanned cells (*y*-axis, cell count). The black region represents the unstimulated cells, and the region surrounded by the red line represents the ATP-stimulated cells. The bar graph on the right side shows the ratio of the mean of fluorescent intensity of ATP-stimulated cells to that of unstimulated cells after treatment with each inhibitor. Data are means ± SD of three independent experiments. $^{**}P < 0.01$, Student's *t*-test.

LY294002 with a Dunn chemotaxis chamber. Microglial chemotaxis toward the higher concentration of ATP was evaluated by analysis of time-lapse images. When 50 μM ATP was applied to the outer well, the cells migrated toward higher concentrations of ATP. Pretreatment of the microglia with wortmannin or LY294002 significantly blocked the chemotaxis (Fig. 1A). The chemotactic movement of the microglia was quantified by calculating the (*x*, *y*) distances individual cells migrated toward ATP. As shown in Fig. 1B, the mean distance migrated by cells pretreated with PI3K inhibitors was significantly shorter than the distance migrated by cells pretreated with DMSO. Treatment with 1 μM AR-C69931MX also inhibited the chemotaxis, as expected based on the results of our previous study (Honda et al., 2001). These findings suggested that PI3K activation is necessary for ATP-induced microglial chemotaxis.

Next, we investigated the effect of PI3K inhibitors on ATP-induced microglial membrane ruffling. As shown in Fig. 2A, phalloidin staining clearly demonstrated that ATP stimulation caused membrane ruffling within 5 min. Pretreatment of microglia with AR-C69931MX inhibited the ATP-induced membrane ruffling, as reported previously (Honda et al., 2001). However, exposure to 100 nM wortmannin or 50 μM LY294002 appeared to have no effect on the membrane ruffling. To confirm the effect of PI3K inhibitors on membrane ruffling quantitatively, the increase in F-actin in cells with membrane ruffles was analyzed with a laser scanning cytometer (LSC), which is a microscope-based cytometer. ATP-stimulated and unstimulated cells were stained with an anti-Iba1 antibody and Alexa Fluor 647-conjugatde phalloidin, and F-actin content was quantified by calculating the mean Alexa Fluor 647 fluorescent intensity of individual cells positive for a microglial marker protein Iba1 (Ito et al., 1998). As shown in Fig. 2B, the mean fluorescent intensity of control microglia was increased approximately 2-fold by ATP stimulation. The fluorescent intensity of ATP-stimulated cells pretreated with AR-C69931MX did not change significantly; however, the fluorescent intensity of cells pretreated with wortmannin or LY294002 was increased by ATP stimulation the same as in the control and the DMSO-treated cells. These results indicate that PI3K activation is not required for the membrane ruffling, but is necessary for induction of microglial chemotaxis.

ATP-Induced Akt Phosphorylation and Effect of Extracellular Calcium Deprivation

To determine whether the PI3K pathway in microglia is activated by ATP stimulation, we investigated Akt phosphorylation, a downstream signaling for PI3K (Bellacosa et al., 1991; Scheid and Woodgett, 2003), by Western blot analysis with a phospho-specific Akt antibody. ATP stimulation rapidly increased the level of Akt phosphorylation in a time-dependent manner (Fig. 3A), and pretreatment with 1 μM AR-C69931MX or 100 nM wortmannin inhibited the increase in Akt phosphorylation (Figs. 3B,C). These results indicated that ATP induces activation of the PI3K/Akt cascade in microglia and that the activation is mediated by P2Y$_{12}$R.

Previous studies (Inoue et al., 1998; Tsuda et al., 2003) have shown that stimulation of microglia with 50 μM ATP induces a transient increase in $[Ca^{2+}]_i$ that depends on the presence of extracellular Ca^{2+}, suggesting that ionotropic P2X receptors are responsible for the Ca^{2+} response. Use of the Ca^{2+}-sensitive fluorescent dye fura-2 revealed that the chelation of extracellular Ca^{2+} suppressed the ATP (50 μM)-evoked increase in $[Ca^{2+}]_i$ in our cultured microglia (data not shown). To determine whether the increase in $[Ca^{2+}]_i$ had any effect on the PI3K/Akt activation, we investigated Akt phosphorylation in microglia stimulated with 50 μM ATP in the absence of extracellular Ca^{2+}, and as shown in Fig. 4, chelation of extracellular Ca^{2+} by EGTA significantly

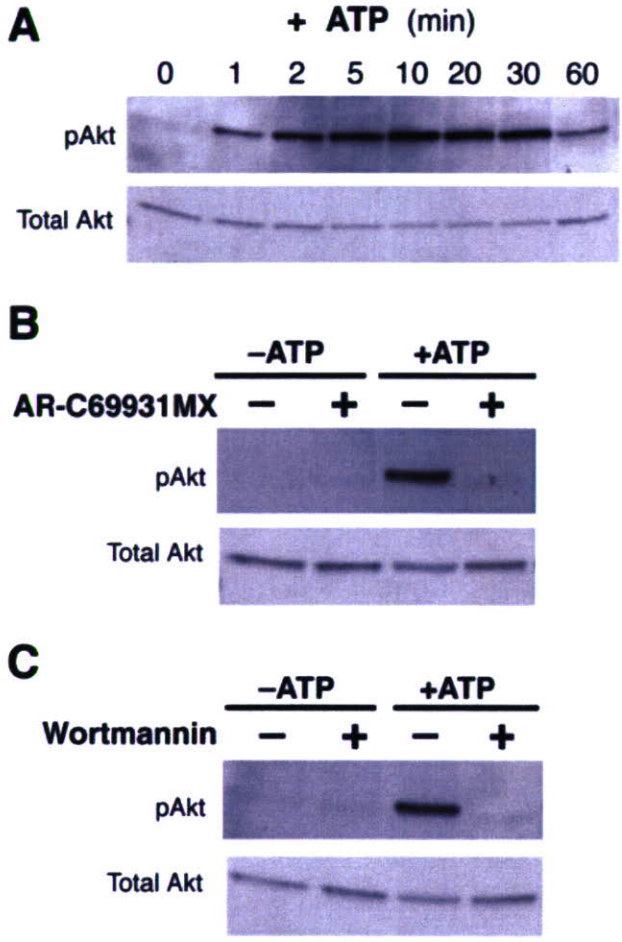

Fig. 3. ATP-induced Akt phosphorylation in microglia is dependent on PI3K activation through P2Y$_{12}$R. (**A**) Microglia were stimulated with 50 μM ATP for the period of time indicated and then lysed in SDS sample buffer. Phosphorylated (pAkt) and total Akt in the lysates were detected by Western blot analysis. (**B**, **C**) Microglia were pretreated with 1 μM AR-C69931MX for 10 min (**B**) or with 100 nM wortmannin for 20 min (**C**) and then stimulated with 50 μM ATP for 5 min. Akt phosphorylation was detected by Western blot analysis. Similar results were obtained from three independent experiments.

decreased ATP-induced Akt phosphorylation. Previous studies have shown that M-CSF stimulates the Fms tyrosine kinase receptor to activate Akt in macrophages in a PI3K-dependent manner (Comalada et al., 2004; Weiss-Haljiti et al., 2004). M-CSF also stimulated Akt phosphorylation in microglia, but chelation of extracellular Ca^{2+} had no effect on it (Fig. 4). These results led us to speculate that the ATP-induced PI3K/Akt activation, which is an essential component for induction of microglial chemotaxis, was linked to an increase in $[Ca^{2+}]_i$ through the extracellular Ca^{2+}-influx via ionotropic P2X receptors.

Effect of P2XR Antagonists on ATP-Induced Microglial Chemotaxis and Akt Phosphorylation

Since primary-cultured microglia have been shown to express P2X$_4$R (Tsuda et al., 2003; Xiang and Burnstock,

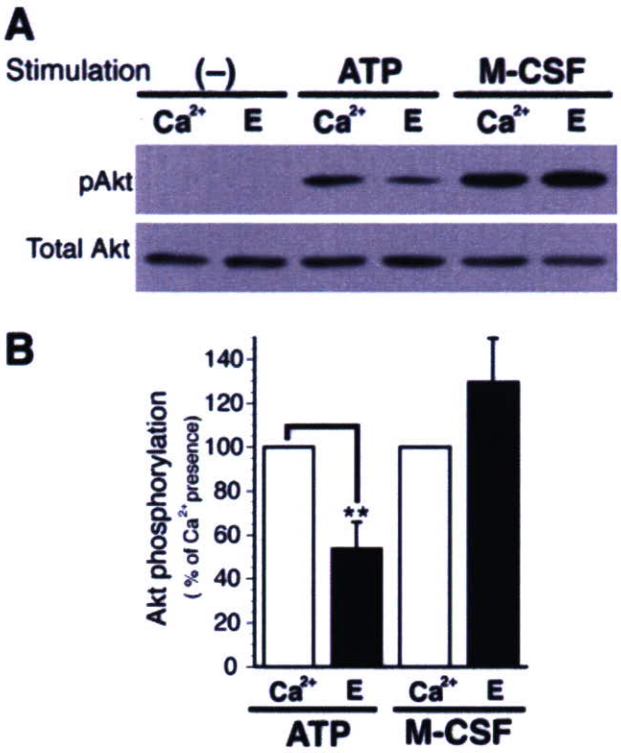

Fig. 4. Inhibitory effect of chelation of extracellular calcium on ATP-stimulated Akt phosphorylation. (**A**) Microglia were incubated for 30 min in BSS containing 1.2 mM Ca^{2+} (Ca^{2+}) or 1 mM EGTA (E) and then stimulated with 50 μM ATP or 100 ng/mL M-CSF for 5 min. Akt phosphorylation was detected by Western blot analysis. (**B**) The Akt phosphorylation level was quantified by densitometry. The results are expressed as percentage of agonist-induced phosphorylation in the presence of Ca^{2+} and are means ± SD of three independent experiments. $^{**}P < 0.01$; Student's *t*-test.

2005) and $P2X_7R$ (Ferrari et al., 1996; Nörenberg et al., 1994; Verkhratsky and Kettenmann, 1996; Walz et al., 1993), we first investigated the involvement of P2XRs in microglial chemotaxis with a $P2X_{1-4}R$, antagonist TNP-ATP, with a $P2X_{1,2,3,5,7}R$ antagonist PPADS, and with a selective $P2X_7R$ antagonist BBG. After pretreatment with an antagonist for 5 min the microglia were observed for chemotactic movement toward ATP in a Dunn chemotaxis chamber containing the antagonist. Treatment with 100 μM TNP-ATP appeared to suppress the ATP-induced microglial chemotaxis, but 300 μM PPADS or 1 μM BBG had no effect (Fig. 5A). The chemotactic movement of the microglia was quantified by calculating the mean value of the total (x, y) distances of individual cells migrated toward ATP. As shown in Fig. 5B, the mean distance migrated by the cells pretreated with TNP-ATP was significantly shorter than the distance migrated by the control cells, but the values of the cells pretreated with PPADS or BBG were not significantly different from those of the controls. Treatment with 1 μM AR-C69931MX also completely inhibited the chemotaxis. These results suggested that $P2X_4R$ as well as $P2Y_{12}R$ is involved in ATP-induced microglial chemotaxis.

We next examined the effect of the three P2XR antagonists, TNP-ATP, PPADS, and BBG, on ATP-stimulated Akt phosphorylation. TNP-ATP significantly suppressed the ATP-stimulated Akt phosphorylation, but PPADS or BBG appeared to have no effect (Fig. 6). AR-C69931MX also completely inhibited Akt phosphorylation. These results suggested that ATP-induced PI3K/Akt activation is mediated by $P2X_4R$ as well as $P2Y_{12}R$.

Downregulation of $P2X_4R$ in Microglia by Short Hairpin $P2X_4R$ RNAi

To determine whether $P2X_4R$ is in fact involved in ATP-induced microglial chemotaxis, we suppressed $P2X_4R$ expression in microglia with RNAi. We constructed a lentivirus vector that expresses both short hairpin (sh)-RNAi and EGFP under the control of the U6 RNA polymerase III promoter and the CMV promoter, respectively (Fig. 7A), and thus cells expressing the shRNAi should also express the EGFP reporter. Microglia were transduced with a lentivirus vector expressing a short hairpin $P2X_4R$ RNAi ($shP2X_4R$) or a control vector that expressed short hairpin luciferase RNAi (shControl). Lentiviral particles were added to mixed glial cell cultures, and floating cells were collected as microglia. To confirm the suppression of $P2X_4R$ expression by $shP2X_4R$, EGFP-positive cells were sorted with a flow cytometer, and expression of $P2X_4R$ protein in the cell lysate was investigated by Western blot analysis with an anti-$P2X_4R$ antibody. $P2X_4R$ protein expression was markedly suppressed in the EGFP-positive cells transduced with $shP2X_4R$ (Fig. 7B), whereas there was no difference in $P2X_4R$ protein level between the EGFP-positive and EGFP-negative cells after transduction with shControl. $P2X_7R$ protein expression was unaffected by transduction with $shP2X_4R$ (Fig. 7B). Microglial RNA was isolated from the sorted cells, and $P2Y_{12}R$ mRNA levels were analyzed by RT-PCR and normalized against actin mRNA levels. $P2Y_{12}R$ mRNA levels increased linearly with PCR reactions for 25–35 cycles. When PCR reactions were performed for 27 cycles, there was no difference in relative level of $P2Y_{12}R$ mRNA in EGFP-positive cells between transduction with $shP2X_4R$ and transduction with shControl (ratio of $P2Y_{12}R$ mRNA level in the $shP2X_4R$-transduced cells to the shControl-transduced cells = 1.1, Fig. 7C). We checked the $P2Y_{12}R$ mRNA level amplified by PCR for 25 and 30 cycles and confirmed that the relative level of $P2Y_{12}R$ mRNA in the $shP2X_4R$-transduced cells was the same as in the shControl-transduced cells. These results indicated that $P2X_4R$ expression was specifically suppressed in the EGFP-positive microglia after transduction with $shP2X_4R$.

The increase in $[Ca^{2+}]_i$ induced by ATP (50 μM) in microglia has been shown to be mediated by $P2X_4R$ (Tsuda et al., 2003). To determine whether $shP2X_4R$ interfered with $P2X_4R$ function in the EGFP-positive microglia, the level of $[Ca^{2+}]_i$ in individual cells was monitored by imaging analysis with fura-2 after transduction with the lentivirus vectors. A 30-s application of 50 μM ATP produced an increase in the 340/380 emission ratio of fura-2 in the EGFP-positive cells transduced with the con-

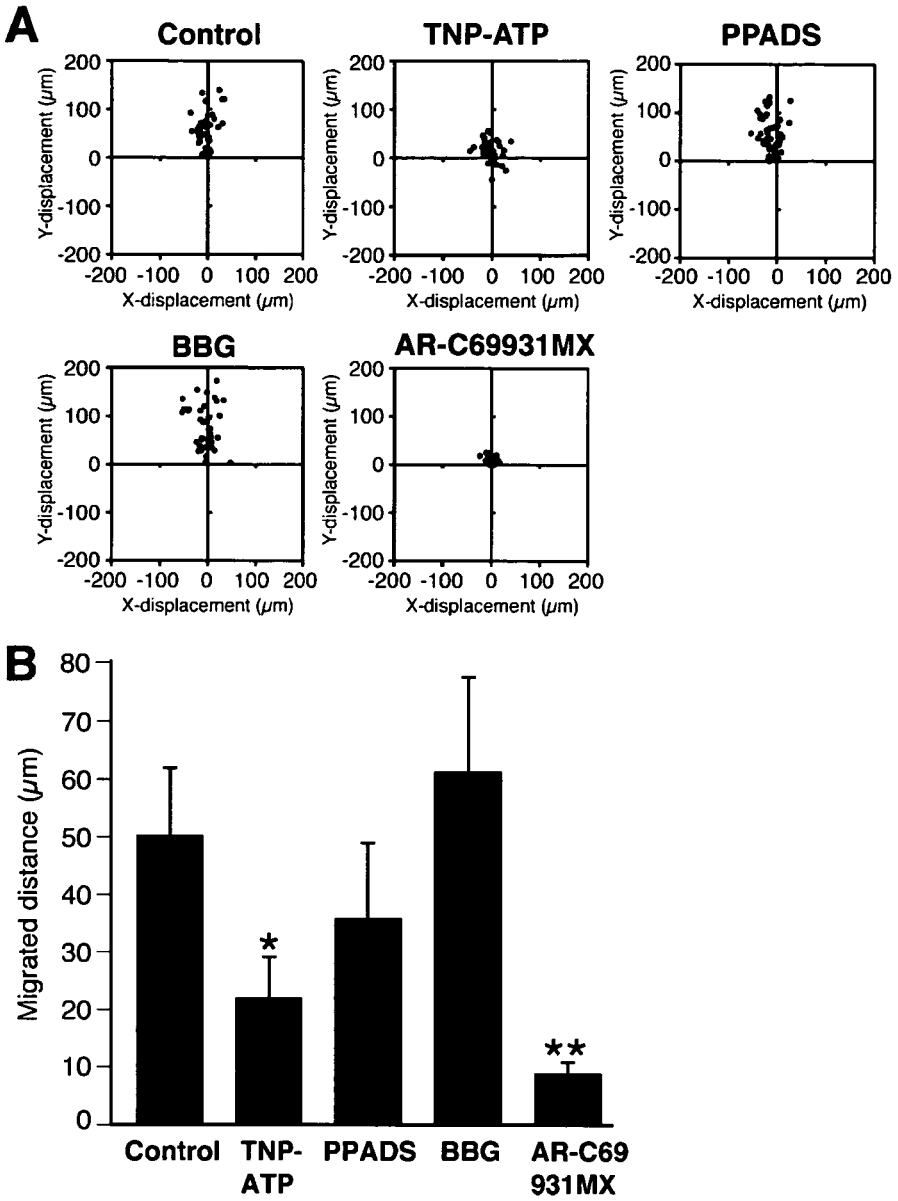

Fig. 5. Effect of P2X antagonists on ATP-induced microglial chemotaxis. (**A**) Microglia were pretreated with 100 μM TNP-ATP, 300 μM PPADS, or 1 μM BBG for 5 min or with 1 μM AR-C69931MX for 10 min. Microglial migration towards 50 μM ATP was observed in the Dunn chemotaxis chamber. The distance and direction of migration by individual cells are shown as x and y coordinates on scatter diagrams. (**B**) Chemotaxis was quantified by measuring the (x, y) distance migrated from the starting position of cells. Data are means ± SD of three independent experiments. $^{*}P < 0.05$, $^{**}P < 0.01$, Student's t-test.

trol vector (Fig. 8A left), whereas the increase in 340/380 emission ratio was significantly attenuated in the EGFP-positive cells transduced with shP2X$_4$R (Figs. 8A,B). These results confirmed that transduction with shP2X$_4$R downregulates expression of P2X$_4$R protein.

Effect of shP2X$_4$R on ATP-Induced Membrane Ruffling and Chemotaxis by Microglia

The effect of P2X$_4$R downregulation on ATP-induced membrane ruffling was examined in microglia transduced with the lentivirus vectors. EGFP-positive cells transduced with shP2X$_4$R or shControl developed membrane ruffles in response to ATP stimulation, the same as EGFP-negative cells (Fig. 9). These results indicated that shP2X$_4$R did not inhibit the activation of P2Y$_{12}$R and suggested that P2X$_4$R downregulation had no effect on ATP-induced membrane ruffling.

The cells transduced with the vectors were also examined for chemotactic movement in a Dunn chemotaxis chamber. As shown in the scatter diagrams, the migration of EGFP-positive cells transduced with shP2X$_4$R (Fig. 10A, bottom left) was clearly inhibited in comparison with the EGFP-negative cells (bottom right). EGFP-positive cells transduced with shControl (top left) migrated toward ATP as same as the EGFP-negative cells (top right). To quantify the effect of the shRNAi on the chemotactic movement of microglia, we calculated the mean value of the (x, y) distances EGFP-positive and -negative cells migrated toward ATP (Fig. 10B). The mean distance migrated by the EGFP-positive cells transduced with shP2X$_4$R was significantly shorter than both the mean distance migrated by the EGFP-negative cells and the mean distance migrated by the EGFP-positive cells

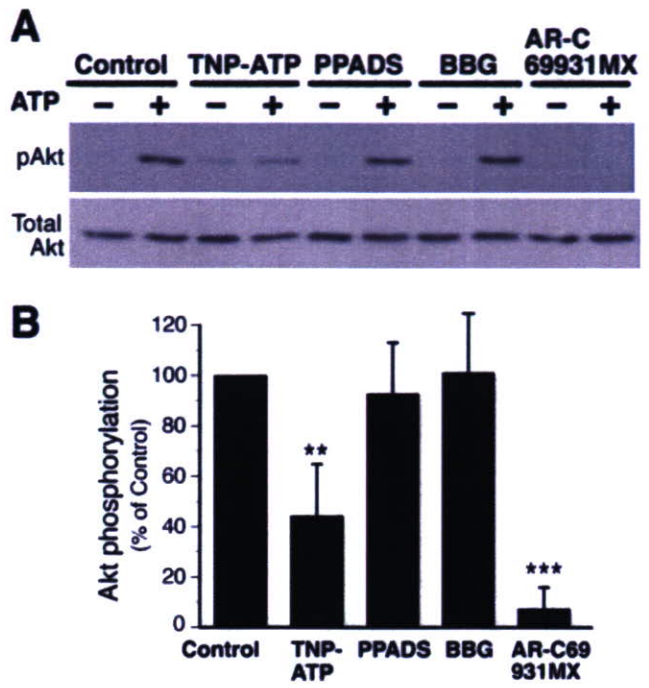

Fig. 6. Effect of P2X antagonists on ATP-stimulated Akt phosphorylation. (**A**) Microglia were pretreated with 100 μM TNP-ATP, 30 μM PPADS, or 100 nM BBG for 5 min or with 1 μM AR-C69931MX for 10 min, and then stimulated with 50 μM ATP for 5 min. Akt phosphorylation was detected by Western blot analysis. (**B**) The Akt phosphorylation level was quantified by densitometry and expressed as percentage of ATP-induced phosphorylation in control cells. The data shown are means ± SD of three independent experiments. $^{**}P < 0.01$, $^{***}P < 0.001$; Student's *t*-test.

transduced with shControl. There was no difference in distance migrated by the EGFP-positive cells and the EGFP-negative cells after transduction with shControl. These results clearly indicated that $P2X_4R$ is involved in ATP-induced microglial chemotaxis.

DISCUSSION

As expected from our previous findings (Honda et al., 2001), both the ATP-induced microglial membrane ruffling and chemotaxis were completely inhibited by a specific $P2Y_{12}R$ antagonist, AR-C69931MX, (Figs. 1 and 2). In this study we further investigated the signaling pathway downstream for $P2Y_{12}R$ and the effect of P2XR antagonists and shRNAi against $P2X_4R$ on microglial migration, and we found that $P2X_4R$ is also involved in ATP-induced microglial chemotaxis.

$P2Y_{12}R$ was known to be coupled to activation of PI3K and inhibition of adenylate cyclase (Czajkowski et al., 2004; Soulet et al., 2004; Van Kolen and Slegers, 2004), and Nasu-Tada et al. (2005) recently reported that a $P2Y_{12}R$-mediated decrease in cyclic AMP is an important step in membrane ruffling and chemotaxis by microglia on fibronectin-coated dishes. PI3K is well known to be a key player in remodeling of the actin cytoskeleton and in regulating cell migration, including chemotaxis (Procko and McColl, 2005; Van Haastert and Devreotes, 2004). In this study we showed that PI3K inhibitors

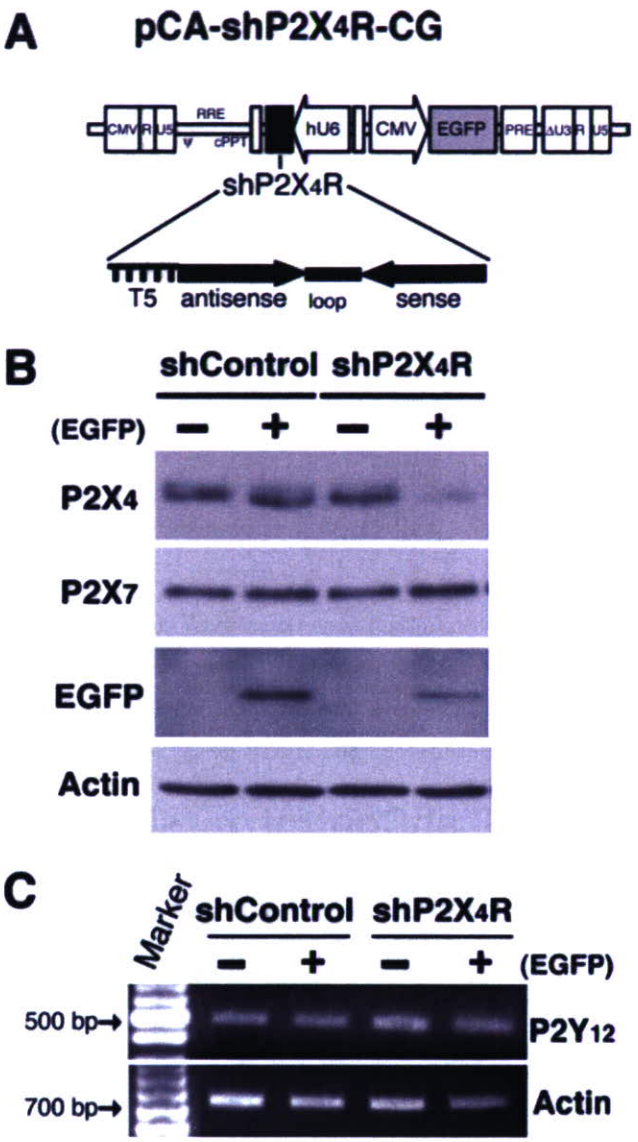

Fig. 7. shRNAi-targeted downregulation of $P2X_4R$ in microglia by lentivirus vectors. (**A**) Schematic drawing of lentivirus vectors expressing EGFP and shRNAi against $P2X_4R$ ($shP2X_4R$). A shRNA sequence targeted for firefly luciferase (shControl) was used as a control. (**B**) Protein expression of $P2X_4R$ and $P2X_7R$ in the microglia transduced with the shRNAi lentivirus vectors. EGFP-positive (+) and -negative (−) cells were sorted with a flow cytometer and lysed in SDS sample buffer. Protein expression of $P2X_4R$, $P2X_7R$, EGFP, and actin in the cell lysates was detected by Western blot analysis. Actin served as an internal control. (**C**) Gene transcript analysis of microglia transduced with the shControl or $shP2X_4R$ vector. RNA was isolated from the sorted cells. Gene transcripts for $P2Y_{12}R$ and β-actin, which served as an internal control, were analyzed by RT-PCR. The relative intensity of the bands for $P2Y_{12}R$ was quantified by densitometry and normalized to the β-actin products. Similar results were obtained from at least three independent experiments.

blocked microglial chemotaxis towards ATP (Fig. 1). However, the PI3K inhibitors had no effect on membrane ruffling (Fig. 2), suggesting that the initial actin reorganization induced by ATP is not dependent on PI3K activation, whereas the ATP gradient-dependent cell migration requires PI3K activation. PI3Ks phosphorylate phosphoinositides at the 3-hydroxyl of the inositol

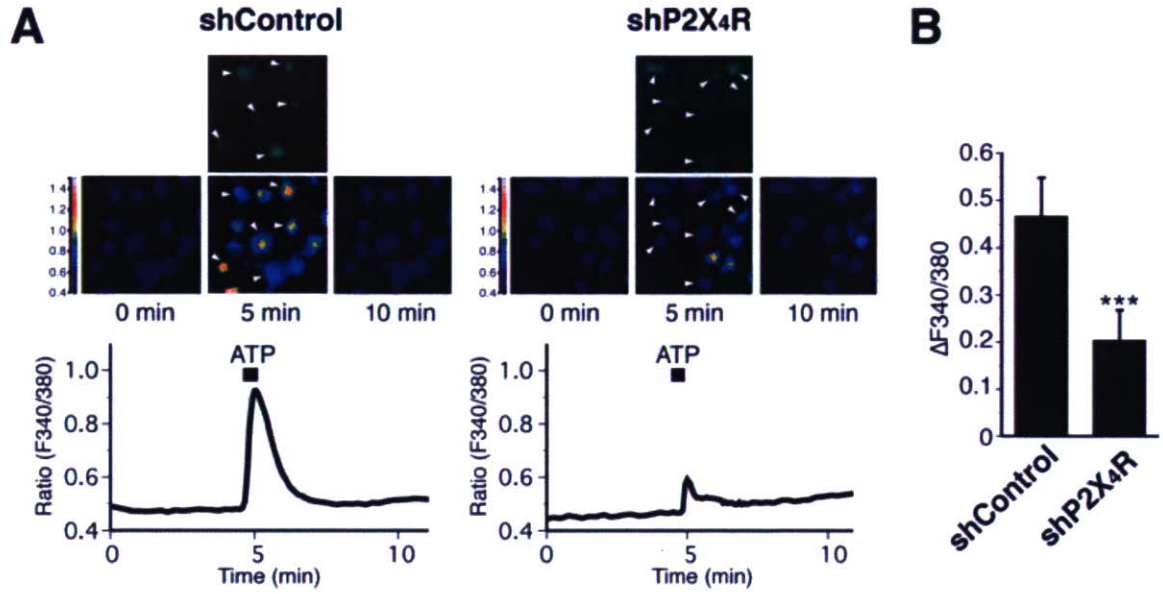

Fig. 8. Effect of P2X$_4$R downregulation on the ATP-evoked increase in $[Ca^{2+}]_i$ in microglia. (**A**) Microglia transduced with the shControl (left panel) or shP2X$_4$R (right panel) vector were loaded with fura-2/AM. $[Ca^{2+}]_i$ was expressed as the ratio of the fluorescence intensity at 340 nm to the fluorescence intensity at 380 nm (F340/380). The pseudocolor image shows three frames (0, 5, and 10 min) of fura2-loaded microglia stimulated with 50 μM ATP for 30 s. Arrowheads point to EGFP-positive cells. The traces show the mean increase in F340/380 emission ratio of 14 EGFP-positive cells from each culture. (**B**) The graphs show the relative increase in ratio (ΔF340/380; mean ± SD, n = 14 cells) from the basal level of the EGFP-positive cells shown in Fig. 8A. $^{***}P < 0.001$; Student's t-test. Similar results were obtained from three independent experiments.

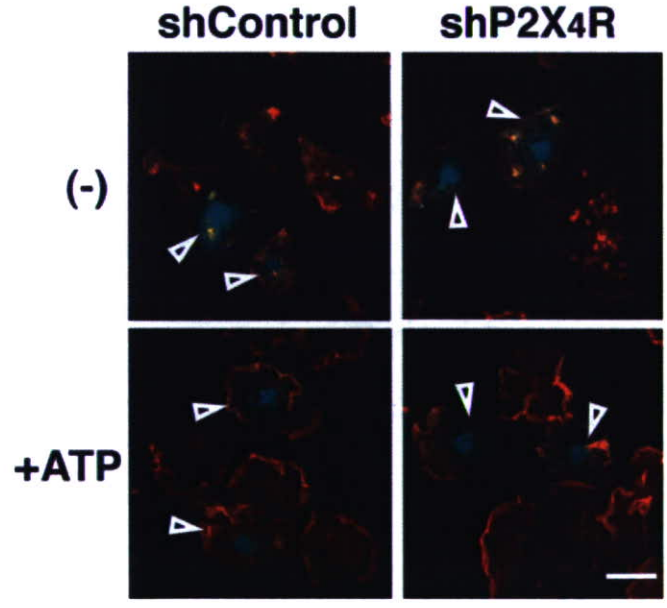

Fig. 9. Effect of P2X$_4$R downregulation on ATP-induced membrane ruffling of microglia. Microglia transduced with the lentivirus vectors were stimulated with 50 μM ATP for 5 min. After fixation, the cells were stained with Texas Red-conjugated phalloidin. Arrowheads indicate EGFP-positive cells. ATP-stimulated membrane ruffling of EGFP-positive cells were observed in three independent experiments. Scale bar, 20 μm.

ring (Vanhaesebroeck et al., 2001). When cells are placed in a chemoattractant gradient, the phosphorylated phospholipids selectively accumulate at the leading edge and act as a membrane anchor for many PI3K downstream effector proteins with pleckstrin homology (PH) regions, which may regulate directional sensing during chemotaxis (Procko and McColl, 2005; Van Haastert and Devreotes, 2004). PI3K will play a crucial role in both sensing the ATP gradient and determining the cell polarity of the microglia.

Akt is activated through binding of its PH domains to lipid products of PI3K on the plasma membrane (Scheid and Woodgett, 2003). In this study ATP-induced increase in Akt phosphorylation was suppressed by pretreatment with a P2Y$_{12}$R antagonist or PI3K inhibitors (Fig. 3). These findings indicated that Akt is phosphorylated following PI3K activation downstream of P2Y$_{12}$R in microglia. Interestingly, the increase in the Akt phosphorylation was suppressed by chelation of extracellular calcium with EGTA (Fig. 4), and depletion of intracellular calcium by BAPTA-AM also blocked the Akt phosphorylation (data not shown). These results indicate that activation of the PI3K-Akt signal pathway is regulated by an increase in $[Ca^{2+}]_i$. Previous studies have shown that in some cells an increase in $[Ca^{2+}]_i$ can activate Akt through PI3K-dependent or independent pathways. An increase in $[Ca^{2+}]_i$ can also activate Src or proline-rich/Ca^{2+}-activated tyrosine kinase Pyk2, thereby directly or indirectly regulating the PI3K activation (Chen et al., 2001; Gendron et al., 2003; Okuda et al., 1999). Protein kinase C (PKC) or Ca^{2+}/calmodulin-dependent protein kinase which is activated by calcium, lies upstream of Akt or directly phosphorylates Akt (Bauer et al., 2003; Gliki et al., 2002; Tanaka et al., 2003; Yano et al., 1998). Further investigation is needed to determine how the calcium signaling regulates the PI3K/Akt activation in microglia.

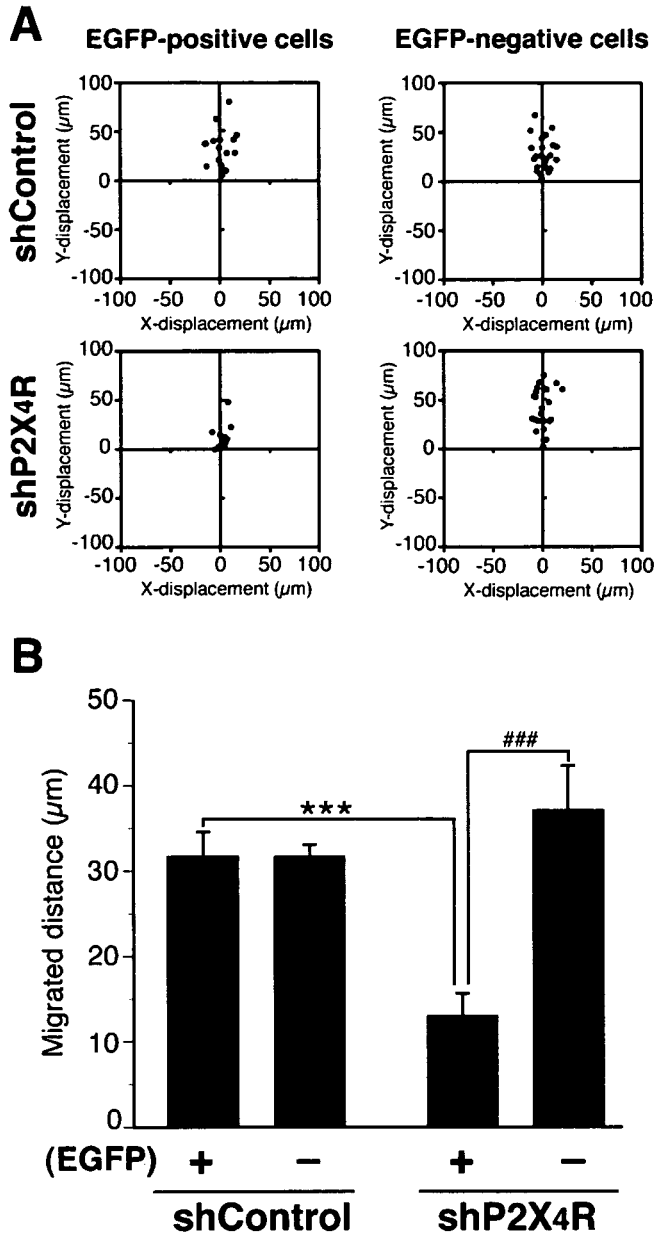

Fig. 10. Inhibitory effect of $P2X_4R$ downregulation on ATP-induced microglial chemotaxis. (**A**) Microglia were transduced with the lentivirus vectors and microglial migration towards 50 μM ATP was observed in the Dunn chemotaxis chamber. The distance and direction of movement by individual cells are shown as x and y coordinates on scatter diagrams. (**B**) Each chemotaxis was quantified by measuring the (x, y) distance migrated from the starting position of cells. Data are means ± SD of three independent experiments. $^{***}P < 0.001$, Student's t-test, compared with shControl EGFP-positive cells; $^{###}P < 0.001$, compared with shP2X4R EGFP-negative cells.

The ATP-induced increase in $[Ca^{2+}]_i$ in microglia has been shown to be suppressed by chelation of extracellular calcium or pretreatment with TNP-ATP, but not by PPADS or BBG (Tsuda et al., 2003). The present study showed that shRNA-mediated downregulation of $P2X_4R$ in microglia suppressed the ATP-induced increase in $[Ca^{2+}]_i$ (Fig. 8). These observations suggest that the increase in $[Ca^{2+}]_i$ is mainly caused by the influx of extracellular calcium through $P2X_4R$. ATP-induced PI3K/Akt activation was inhibited by pretreatment with TNP-ATP, but not with PPADS or BBG (Fig. 6). Interference with $P2X_4R$ expression markedly inhibited the ATP-induced microglial chemotaxis (Fig. 10) without affecting membrane ruffling (Fig. 9), the same as the effects of PI3K inhibitors (Figs. 1 and 2). We therefore suspect that the $P2X_4R$-mediated calcium signaling may be involved in PI3K/Akt activation and regulate microglial chemotaxis. Local Ca^{2+} mobilization through $P2X_4R$ at membrane ruffles may be necessary for maintenance or enhancement of the local $P2Y_{12}R$-activated PI3K signals.

Membrane ruffling is generated by dynamic remodeling of the actin cytoskeleton at the plasma membrane and is thought to be a crucial process for cell migration (Small et al., 2002). $P2Y_{12}R$ activation is essential for ATP-induced membrane ruffling and triggers intracellular signaling events that lead to microglial chemotaxis toward ATP. Ca^{2+} imaging showed that shP2×4R did not completely suppress the ATP-evoked increase in $[Ca^{2+}]_i$ (Fig. 9), suggesting that other subtypes of ATP receptor are involved in the Ca^{2+} response. P2Y receptors are generally linked to activation of phospholipase C (PLC) that catalyzes the hydrolysis of phosphatidylinositol 4,5-bisphosphate to the intracellular messenger inositol 1,4,5, triphosphate (IP_3) and diacylglycerol (Communi et al., 2000). ATP-stimulated $P2Y_{12}R$ will induce PLC activation, leading to IP_3-mediated Ca^{2+} release from intracellular calcium stores in microglia. P2Y receptors modulate G-protein coupled or voltage-dependent ion channels that affect the Ca^{2+} current (Van Kolen and Slegers, 2006). Vial et al. (2002) reported that coactivation of $P2X_1R$ and $P2Y_1R$ in platelets synergistically enhances the Ca^{2+} response and suggested that $P2X_1$ may have a priming role in the activation of $P2Y_1R$ during platelet activation. Further study is needed to analyze cross-talk between $P2X_4R$ and other signal pathways downstream of $P2Y_{12}R$, such as the adenylate cyclase pathway or PLC pathway.

$P2Y_{12}R$ is constitutively expressed in microglia in the normal brain (Sasaki et al., 2003). A recent report by Haynes et al. (2006) shows that $P2Y_{12}R$ is essential for early microglial responses towards either a local ATP injection or a focal laser injury in brain slices. $P2Y_{12}R$ play crucial roles in regulating the morphological changes in ramified microglia and cell migration by activated microglia in response to ATP released by surrounding cells and its hydrolysis product ADP. By contrast, $P2X_4R$ expression in microglia is lower in the normal brain and spinal cord, and it is significantly upregulated in activated microglia within 24 h after ischemia or nerve injury (Cavaliere et al., 2003; Schwab et al., 2005; Zhang et al., 2006). Tsuda et al. (2003) recently reported that the $P2X_4R$ expression is induced in spinal microglia during the tactile allodynia observed after nerve injury. These observations together with our own findings suggest that $P2X_4R$ activation may modulate or enhance the microglial cell migration in pathological conditions. Although further study is needed to clarify the molecular mechanisms underlying the microglial cell migration

mediated by $P2Y_{12}R$ and $P2X_4R$, the findings in the present study may contribute to understanding the ATP-induced changes in microglial dynamics in the brain in normal and pathological states.

ACKNOWLEDGMENTS

We thank Dr. Miyoshi (Bio Resource Center, RIKEN, Tsukuba, Japan) for providing us with lentivirus vector system, and Dr. Shin'ichi Takeda, Dr. Hirohiko Hojoh, and Mr. Masuda Satoshi (National Institute of Neuroscience) for their advice and technical support.

REFERENCES

Bauer B, Jenny M, Fresser F, Uberall F, Baier G. 2003. AKT1/PKBα is recruited to lipid rafts and activated downstream of PKC isotypes in CD3-induced T cell signaling. FEBS Lett 541:155–162.

Bellacosa A, Testa JR, Staal SP, Tsichlis PN. 1991. A retroviral oncogene, akt, encoding a serine–threonine kinase containing an SH2-like region. Science 254:274–277.

Cavaliere F, Florenzano F, Amadio S, Fusco FR, Viscomi MT, D'Ambrosi N, Vacca F, Sancesario G, Bernardi G, Molinari M, Volonte C. 2003. Up-regulation of $P2X_2$, $P2X_4$ receptor and ischemic cell death: Prevention by P2 antagonists. Neuroscience 120:85–98.

Chen R, Kim O, Yang J, Sato K, Eisenmann KM, McCarthy J, Chen H, Qiu Y. 2001. Regulation of Akt/PKB activation by tyrosine phosphorylation. J Biol Chem 276:31858–31862.

Comalada M, Xaus J, Sanchez E, Valledor AF, Celada A. 2004. Macrophage colony-stimulating factor-, granulocyte–macrophage colony-stimulating factor-, or IL-3-dependent survival of macrophages, but not proliferation, requires the expression of p21(Wafl) through the phosphatidylinositol 3-kinase/Akt pathway. Eur J Immunol 34:2257–2267.

Communi D, Janssens R, Suarez-Huerta N, Robaye B, Boeynaems JM. 2000. Advances in signalling by extracellular nucleotides. The role and transduction mechanisms of P2Y receptors. Cell Signal 12:351–360.

Czajkowski R, Banachewicz W, Ilnytska O, Drobot LB, Baranska J. 2004. Differential effects of $P2Y_1$ and $P2Y_{12}$ nucleotide receptors on ERK1/ERK2 and phosphatidylinositol 3-kinase signalling and cell proliferation in serum-deprived and nonstarved glioma C6 cells. Br J Pharmacol 141:497–507.

Davalos D, Grutzendler J, Yang G, Kim JV, Zuo Y, Jung S, Littman DR, Dustin ML, Gan WB. 2005. ATP mediates rapid microglial response to local brain injury in vivo. Nat Neurosci 8:752–758.

Ferrari D, Villalba M, Chiozzi P, Falzoni S, Ricciardi-Castagnoli P, Di Virgilio F. 1996. Mouse microglial cells express a plasma membrane pore gated by extracellular ATP. J Immunol 156:1531–1539.

Gendron FP, Neary JT, Theiss PM, Sun GY, Gonzalez FA, Weisman GA. 2003. Mechanisms of $P2X_7$ receptor-mediated ERK1/2 phosphorylation in human astrocytoma cells. Am J Physiol Cell Physiol 284: C571–C581.

Gliki G, Wheeler-Jones C, Zachary I. 2002. Vascular endothelial growth factor induces protein kinase C (PKC)-dependent Akt/PKB activation and phosphatidylinositol 3/-kinase-mediates PKC δ phosphorylation: Role of PKC in angiogenesis. Cell Biol Int 26:751–759.

Haynes SE, Hollopeter G, Yang G, Kurpius D, Dailey ME, Gan WB, Julius D. 2006. The P2Y(12) receptor regulates microglial activation by extracellular nucleotides. Nat Neurosci 12:1512–1519.

Honda S, Sasaki Y, Ohsawa K, Imai Y, Nakamura Y, Inoue K, Kohsaka S. 2001. Extracellular ATP or ADP induce chemotaxis of cultured microglia through Gi/o-coupled P2Y receptors. J Neurosci 21:1975–1982.

Illes P, Alexandre Ribeiro J. 2004. Molecular physiology of P2 receptors in the central nervous system. Eur J Pharmacol 483:5–17.

Imai Y, Ibata I, Ito D, Ohsawa K, Kohsaka S. 1996. A novel gene iba1 in the major histocompatibility complex class III region encoding an EF hand protein expressed in a monocytic lineage. Biochem Biophys Res Commun 224:855–862.

Inoue K. 2002. Microglial activation by purines and pyrimidines. Glia 40:156–163.

Inoue K, Nakajima K, Morimoto T, Kikuchi Y, Koizumi S, Illes P, Kohsaka S. 1998. ATP stimulation of Ca^{2+}-dependent plasminogen release from cultured microglia. Br J Pharmacol 123:1304–1310.

Ito D, Imai Y, Ohsawa K, Nakajima K, Fukuuchi Y, Kohsaka S. 1998. Microglia-specific localisation of a novel calcium binding protein, Iba1. Brain Res Mol Brain Res 57:1–9.

James G, Butt AM. 2002. P2Y and P2X purinoceptor mediated Ca^{2+} signalling in glial cell pathology in the central nervous system. Eur J Pharmacol 447:247–260.

Kreutzberg GW. 1996. Microglia: A sensor for pathological events in the CNS. Trends Neurosci 19:312–318.

Moran LB, Graeber MB. 2004. The facial nerve axotomy model. Brain Res Brain Res Rev 44:154–178.

Nakajima K, Kohsaka S. 2005.Response of microglia to brain injury. In: Kettenmann H, Ransom BR, editors. Neuroglia. New York: Oxford University Press. pp 443–453.

Nakajima K, Shimojo M, Hamanoue M, Ishiura S, Sugita H, Kohsaka S. 1992. Identification of elastase as a secretory protease from cultured rat microglia. J Neurochem 58:1401–1408.

Nasu-Tada K, Koizumi S, Inoue K. 2005. Involvement of β1 integrin in microglial chemotaxis and proliferation on fibronectin: Different regulations by ADP through PKA. Glia 52:98–107.

Nimmerjahn A, Kirchhoff F, Helmchen F. 2005. Resting microglial cells are highly dynamic surveillants of brain parenchyma in vivo. Science 308:1314–1318.

Nishitsuji H, Ikeda T, Miyoshi H, Ohashi T, Kannagi M, Masuda T. 2004. Expression of small hairpin RNA by lentivirus-based vector confers efficient and stable gene-suppression of HIV-1 on human cells including primary non-dividing cells. Microbes Infect 6: 76–85.

Nörenberg W, Langosch JM, Gebicke-Haerter PJ, Illes P. 1994. Characterization and possible function of adenosine 5/-triphosphate receptors in activated rat microglia. Br J Pharmacol 111:942–950.

Okuda M, Takahashi M, Suero J, Murry CE, Traub O, Kawakatsu H, Berk BC. 1999. Shear stress stimulation of p130(cas) tyrosine phosphorylation requires calcium-dependent c-Src activation. J Biol Chem 274:26803–26809.

Procko E, McColl SR. 2005. Leukocytes on the move with phosphoinositide 3-kinase and its downstream effectors. Bioessays 27:153–163.

Ralevic V, Burnstock G. 1998. Receptors for purines and pyrimidines. Pharmacol Rev 50:413–492.

Ridley AJ. 2001. Rho proteins, PI 3-kinases, and monocyte/macrophage motility. FEBS Lett 498:168–171.

Sasaki Y, Hoshi M, Akazawa C, Nakamura Y, Tsuzuki H, Inoue K, Kohsaka S. 2003. Selective expression of Gi/o-coupled ATP receptor $P2Y_{12}$ in microglia in rat brain. Glia 44:242–250.

Scheid MP, Woodgett JR. 2003. Unravelling the activation mechanisms of protein kinase B/Akt. FEBS Lett 546:108–112.

Schwab JM, Guo L, Schluesener HJ. 2005. Spinal cord injury induces early and persistent lesional $P2X_4$ receptor expression. J Neuroimmunol 163:185–189.

Small JV, Stradal T, Vignal E, Rottner K. 2002. The lamellipodium: Where motility begins. Trends Cell Biol 12:112–120.

Soulet C, Sauzeau V, Plantavid M, Herbert JM, Pacaud P, Payrastre B, Savi P. 2004. Gi-dependent and -independent mechanisms downstream of the $P2Y_{12}$ ADP-receptor. J Thromb Haemost 2:135–146.

Stence N, Waite M, Dailey ME. 2001. Dynamics of microglial activation: A confocal time-lapse analysis in hippocampal slices. Glia 33:256–266.

Streit WJ. 2002. Microglia as neuroprotective, immunocompetent cells of the CNS. Glia 40:133–139.

Tanaka Y, Gavrielides MV, Mitsuuchi Y, Fujii T, Kazanietz MG. 2003. Protein kinase C promotes apoptosis in LNCaP prostate cancer cells through activation of p38 MAPK and inhibition of the Akt survival pathway. J Biol Chem 278:33753–33762.

Tsuda M, Shigemoto-Mogami Y, Koizumi S, Mizokoshi A, Kohsaka S, Salter MW, Inoue K. 2003. $P2X_4$ receptors induced in spinal microglia gate tactile allodynia after nerve injury. Nature 424:778–783.

Van Haastert PJ, Devreotes PN. 2004. Chemotaxis: Signalling the way forward. Nat Rev Mol Cell Biol 5:626–634.

Vanhaesebroeck B, Leevers SJ, Ahmadi K, Timms J, Katso R, Driscoll PC, Woscholski R, Parker PJ, Waterfield MD. 2001. Synthesis and function of 3-phosphorylated inositol lipids. Annu Rev Biochem 70:535–602.

Van Kolen K, Slegers H. 2004. $P2Y_{12}$ receptor stimulation inhibits β-adrenergic receptor-induced differentiation by reversing the cyclic AMP-dependent inhibition of protein kinase B. J Neurochem 89:442–453.

Van Kolen K, Slegers H. 2006. Integration of P2Y receptor-activated signal transduction pathways in G protein-dependent signaling networks. Purinergic Signalling 2:451–469.

Vial C, Rolf MG, Mahaut-Smith MP, Evans RJ. 2002. A study of P2X1 receptor function in murine megakaryocytes and human platelets reveals synergy with P2Y receptors. Br J Pharmacol 135:363–372.

Verkhratsky A, Kettenmann H. 1996. Calcium signalling in glial cells. Trends Neurosci 19:346–352.

Walz W, Ilschner S, Ohlemeyer C, Banati R, Kettenmann H. 1993. Extracellular ATP activates a cation conductance and a K^+ conductance in cultured microglial cells from mouse brain. J Neurosci 13:4403–4411.

Webb SE, Pollard JW, Jones GE. 1996. Direct observation and quantification of macrophage chemoattraction to the growth factor CSF-1. J Cell Sci 109:793–803.

Weiss-Haljiti C, Pasquali C, Ji H, Gillieron C, Chabert C, Curchod ML, Hirsch E, Ridley AJ, van Huijsduijnen RH, Camps M, Rommel C. 2004. Involvement of phosphoinositides 3-kinase γ, Rac, and PAK signaling in chemokine-induced macrophage migration. J Biol Chem 279:43273–43284.

Xiang Z, Burnstock G. 2005. Expression of P2X receptors on rat microglial cells during early development. Glia 52:119–126.

Yano S, Tokumitsu H, Soderling TR. 1998. Calcium promotes cell survival through CaM-K kinase activation of the protein-kinase-B pathway. Nature 396:584–587.

Yogosawa S, Hatakeyama S, Nakayama KI, Miyoshi H, Kohsaka S, Akazawa C. 2005. Ubiquitylation and degradation of serum-inducible kinase by hVPS18, a RING-H2 type ubiquitin ligase. J Biol Chem 280: 41619–41627.

Zhang Z, Artelt M, Burnet M, Trautmann K, Schluesener HJ. 2006. Lesional accumulation of $P2X_4$ receptor monocytes following experimental traumatic brain injury. Exp Neurol 197:252–257.